

Virtual screening based on molecular docking of lysosomotropic compounds as therapeutic agents for COVID-19

Triagem virtual baseada no encaixe molecular de compostos lisossomotrópicos como agentes terapêuticos para COVID-19

João Batista de Andrade Neto^{1,4,5} , Emanuelle Machado Marinho² , Cecília Rocha da Silva^{1,5} , Lívia Gurgel do Amaral Valente Sá^{4,5} , Vitória Pessoa de Farias Cabral^{1,4} , Thiago Mesquita Cândido¹ , Wildson Max Barbosa da Silva⁴ , Letícia Bernardo Barbosa⁴ , Bruno Coelho Cavalcanti⁵ , Pedro de Lima-Neto² , Emmanuel Silva Marinho³ , Akenaton Onassis Cardoso Viana Gomes⁴ , Hélio Vitoriano Nobre Júnior^{1,5} 

1. School of Pharmacy, Laboratory for Bioprospection of Antimicrobial Molecules (LABIMAN), Federal University of Ceará, Fortaleza, CE, Brazil. 2. Department of Analytical Chemistry and Physical Chemistry, Group of Theoretical Chemistry (GQT), Science Center, Federal University of Ceará, Fortaleza-CE, 60.455-760, Brazil. 3. Department of Chemistry, Group for Theoretical Chemistry and Electrochemistry (GQTE), State University of Ceará, Limoeiro do Norte, Ceará, Brazil. 4. Christus University Center (UNICHRISTUS), Fortaleza, Ceará, Brazil. 5. Drug Research and Development Center, Federal University of Ceará, Fortaleza, CE, Brazil.

Abstract

Objective: Analyze lysosomotropic agents and their action on COVID-19 targets using the molecular docking technique. **Methods:** Molecular docking analyses of these lysosomotropic agents were performed, namely of fluoxetine, imipramine, chloroquine, verapamil, tamoxifen, amitriptyline, and chlorpromazine against important targets for the pathogenesis of SARS-CoV-2. **Results:** The results revealed that the inhibitors bind to distinct regions of Mpro COVID-19, with variations in RMSD values from 1.325 to 1.962 Å and binding free energy of -5.2 to -4.3 kcal/mol. Furthermore, the analysis of the second target showed that all inhibitors bonded at the same site as the enzyme, and the interaction resulted in an RMSD variation of 0.735 to 1.562 Å and binding free energy ranging from -6.0 to -8.7 kcal/mol. **Conclusion:** Therefore, this study allows proposing the use of these lysosomotropic compounds. However, these computer simulations are just an initial step toward conceiving new projects for the development of antiviral molecules.

Keywords: Lysosomotropic agents; SARS-CoV; Molecular Docking.

Resumo

Objetivo: Analisar agentes lisossomotrópicos e sua ação em alvos de COVID-19 usando a técnica de docking molecular. **Métodos:** Foram realizadas análises de docagem molecular destes agentes lisossomotrópicos, nomeadamente de fluoxetina, imipramina, cloroquina, verapamil, tamoxifeno, amitriptilina e clorpromazina contra alvos importantes para a patogenia do SARS-CoV-2. **Resultados:** Os resultados revelaram que os inibidores se ligam a regiões distintas do Mpro COVID-19, com variações nos valores de RMSD de 1.325 a 1.962 Å e energia livre de ligação de -5,2 a -4,3 kcal/mol. Além disso, a análise do segundo alvo mostrou que todos os inibidores se ligaram no mesmo sítio da enzima, e a interação resultante em uma variação de RMSD de 0,735 a 1,562 Å e energia livre de ligação variando de -6,0 a -8,7 kcal/mol. **Conclusão:** Portanto, este estudo permite propor o uso desses compostos lisossomotrópicos. No entanto, essas simulações em computador são apenas um passo inicial para a concepção de novos projetos para o desenvolvimento de moléculas antivirais.

Palavras-chave: Agentes lisossomotrópicos; SARS-CoV; Docagem Molecular.

INTRODUCTION

The World Health Organization declared a global emergency and pandemic due to the new disease called Coronavirus Disease 2019 (COVID-19)^{1,2}. It has become one of the major pathogens affecting the human respiratory system. Along with SARS-CoV (Severe Acute Respiratory Syndrome CoV) and the MERS CoV (Middle East Respiratory Syndrome), it is a great public health threat³. Currently, there are no appropriate vaccines or antiviral agents available that can effectively prevent or treat COVID-19 infection, and mortality is increasing daily. Therefore, effective treatment and control mechanisms are needed to ameliorate the disease's devastating effects⁴. The entry of enveloped viruses such as SARs CoV involves two steps: receptor binding and membrane fusion. The membrane

fusion step by coronavirus spikes requires two cleavages by host proteases, including lysosomal proteases⁵. Therefore, we selected lysosomotropic compounds that, because they are free of lipophilic bases, easily pass through the lipid bilayers and are trapped in the acidic environment of the lysosomes, allowing them to reach large concentrations inside this organelle. Thus, these compounds can prevent the completion of the viral cycle⁶. Because of the global economic recession triggered by the pandemic, the cost of infrastructure for experimental trials is out of reach of most researchers⁷. Therefore, we investigated in silico docking models of the proteins NSP16-NSP10 and their main protease, COVID-19. They can be used as molecular targets for drug discovery.

Correspondence: Hélio Vitoriano Nobre Júnior. Laboratory for Bioprospection of Antimicrobial Molecules (LABIMAN), Federal University of Ceará, Fortaleza, CE, Brazil E-mail: label_ufc@yahoo.com.br

Conflict of interest: The authors declare that there is no conflict of interest.

Received: 2022 Jan 5; Revised: 2022 May 20; Accepted: 2022 Jun 15

MATERIALS AND METHODS

Enzyme Collection and Preparation

The structures were obtained from data deposited in the Protein Data Bank (<https://www.rcsb.org/>): main protease COVID-19 (Mpro), identified in the repository as The crystal structure of COVID-19 main protease in complex with an inhibitor N3, PDB ID: 6LU7, deposited in the Protein Data Bank with the resolution of 2.16 Å, determined from R-Value Free: 0 X-ray diffraction.235, R-Value Work: 0.202, R-Value Observed: 0.204), classified as a viral protein, organism Bat SARS-like coronavirus and expression system Escherichia coli BL21(DE3)⁸. NSP16-NSP10 SARS-CoV-2, identified in the repository as 1.98 Angstrom Resolution Crystal Structure of NSP16-NSP10 Heterodimer from SARS-CoV-2 in Complex with Sinefungin, PDB ID: 6WKQ, the structure is deposited in the Protein Data Bank with the resolution of 1.98 Å, determined from X-ray diffraction (R-Value Free: 0.180, R-Value Work: 0.162), classified as viral protein, organism Severe acute respiratory syndrome coronavirus 2 and expression system Escherichia coli BL21(DE3). In the process of protein preparation, all residues were removed and polar hydrogen was added^{9,10} producing favorable protonation states for molecular docking¹¹.

Obtaining and Preparing Binders

Redirecting approved drugs is an alternative approach to quickly identify potential substances to treat rapidly spreading novel viral infections⁸. All the two-dimensional coordinates of the drugs were obtained from the Pubchem repository (<https://pubchem.ncbi.nlm.nih.gov/>) (Table 1). To obtain the three-dimensional structure in the most stable thermodynamic conformation, the binders were optimized according to an adaptation of the method proposed by Dewar and collaborators¹²⁽¹⁹⁸⁵⁾¹³. At this stage, semi-empirical quantum formalism was used, with the algorithms available in the code of the Molecular Orbital Package (MOPAC, 2016), Version 16.111W^{7,14,15}, which was used for optimization. The parametric method 7 (PM7)¹⁶, with Hartree-Fock (HF) approximation (self-consistent field method), was used for wave function, considering the molecule in the fundamental state and vacuum¹⁵.

Molecular Docking

The simulations were configured to perform continuous calculations of cycles of 500 interactions with a convergence value of 10-10 kcal mol⁻¹¹⁷. In this stage, the conformational stability of the compound is given by the total energy, which is the sum of nuclear repulsive energies and electronic energy. The fitting simulations between the selected inhibitors and proteins were performed using AutoDock Vina code (version 1.1.2), employing 3-way multithreading, Lamarckian Genetic Algorithm [18], with docking parameters: m-pro(center_x = -26.734, center_y = 13.009, center_z = 56.185, size_x = 94, size_y = 112, size_z = 108, spacing = 0.642 and exhaustiveness = 8), NSP16-NSP10 (center_x = 78.486, center_y = -1.045, center_z = -9.341,

size_x = 102, size_y = 126, size_z = 108, spacing = 0.764 and exhaustiveness = 8). As a standard procedure, 100 independent simulations were performed, obtaining 10 poses each, for each targeted protein. As selection criteria, the simulations that presented poses with root mean square deviation (RMSD) values lower than 2,000¹⁹ and free power connection (ΔG) lower than -6.0 kcal/mol²⁰ were analyzed. For result analysis, image plotter and bi- and tridimensional map generation, Discovery Studio Visualizer and UCSF Chimera were used^{7,21}.

RESULTS

Interactions of lysosomotropic compounds with Mpro COVID-19 residues.

Molecular docking routines generated the RMSD values¹⁹ and free binding energy²⁰ between lysosomotropic molecules and Mpro COVID-19 residues. We observed variations in RMSD values from 1.325 to 1.962 Å and free binding energy of -5.2 to -4.3 kcal/mol (Table 1). The analysis of the molecular docking simulations showed that the inhibitors bonded to different regions of the enzyme. Fluoxetine, imipramine, chloroquine, and verapamil remained in the same region as the remdesivir inhibitor (Figure 1). Tamoxifen and amitriptyline were in the same region as azithromycin (Figure 1), while chlorpromazine was in the same region as FJC inhibitor (Figure 1). By comparing the calculated distances between the inhibitors and the residues from the Mpro COVID-19 binding site (Table 2), we noted that all the binders were at a greater distance from the inhibitors (remdesivir, azithromycin, and FJC inhibitor) complexed in the main protease of the COVID-19 virus (Mpro), as shown in Figure 1. The analysis of the interactions showed that fluoxetine (Figure 2) showed seven interactions with Mpro COVID-19, three hydrophobic interactions, with Asp197 (3.74 Å), Thr199 (3.61 Å), and Glu290(3).91 Å), two hydrogen bonds, with Asn238 (2.72 Å; 2.73 Å), both classified as strong²², and two halogens (fluorine) interactions, with the amino acid residue Asp197 (2.52 Å; 3.08 Å) (Table 3). Analysis of the receptor-ligand complex formed with imipramine in the binder (Figure 2) revealed five interactions with the amino acid residues of the enzyme, two hydrophobic interactions, with Lys137 (3.70 Å) and Leu286 (3.54 Å), two hydrogen bond interaction, with Arg131 (3.67 Å) and Thr199 (3.33 Å), both classified as weak²², and one salt bridge interaction, with Asp 197 (4.93 Å) (Table 3). The verapamil inhibitor (Figure 2C) showed five interactions with the main protease of the COVID-19 virus, two hydrophobic interactions, with Lys137 (3.72 Å) and Leu286 (3.88 Å), one π -cation interaction, with Lys137 (4.26 Å), and two salt bridge interactions, with Glu288 (5.28 Å) and Glu290 (5.38 Å) (Table 3). The analysis of interactions with tamoxifen showed that the simulation of the molecular fit of the inhibitor (Figure 2) resulted in the formation of six interactions with the enzyme, five of which were hydrophobic, with the residues Ile249 (3.92 Å, 3.60 Å), Phe294 (3.85 Å) and Val297 (3.88 Å; 3.64 Å), and one salt bridge interaction, with Asp153 (4.37 Å) (Table 3). Amitriptyline (Figure 2E) showed six interactions with the Mpro COVID-19 residues, all of them hydrophobic, with Ile249 (3.96

3 Virtual screening based on molecular docking of lysosomotropic compounds for COVID-19

Å; 3.55 Å), Pro252 (3.58 Å), Pro293 (3.71 Å), Phe294 (3.98 Å) and Val297 (3.67 Å) (Table 3). Chlorpromazine molecular docking routines (Figure 2F) showed the formation of two protein target interactions, both hydrophobic, with Phe140 (3.90 Å) and Glu166 (3.56 Å) (Table 3).

Table 1. RMSD and affinity energy values calculated in molecular docking simulations in the Mpro COVID-19 residues

Inhibitor	Affinity (kcal/mol)	RMSD (Å)
Azithromycin ^b	-5.8	1.253
Inhibitor FJCb	-6.7	1.579
Remdesivir ^b	-6.8	2.058
Chloroquine ^{b,c}	-4.2	1.477
Fluoxetine ^c	-5.0	1.567
Imipramine ^c	-5.2	1.676
Verapamil ^c	-4.9	1.962
Chlorpromazine ^c	-4.8	1.778
Amitriptyline ^c	-5.2	1.878
Tamoxifen ^c	-5.3	1.325

a. The crystal structure of COVID-19 main protease - PDB ID: 6LU7

b. Molecules ligands of COVID-19 main protease described in literature.

c. Lysosomotropic compounds

Figure 1. The lysosomotropic compounds fluoxetine, imipramine, chloroquine, verapamil, tamoxifen, amitriptyline and chlorpromazine binding the Mpro COVID-19 residues compared to N3.

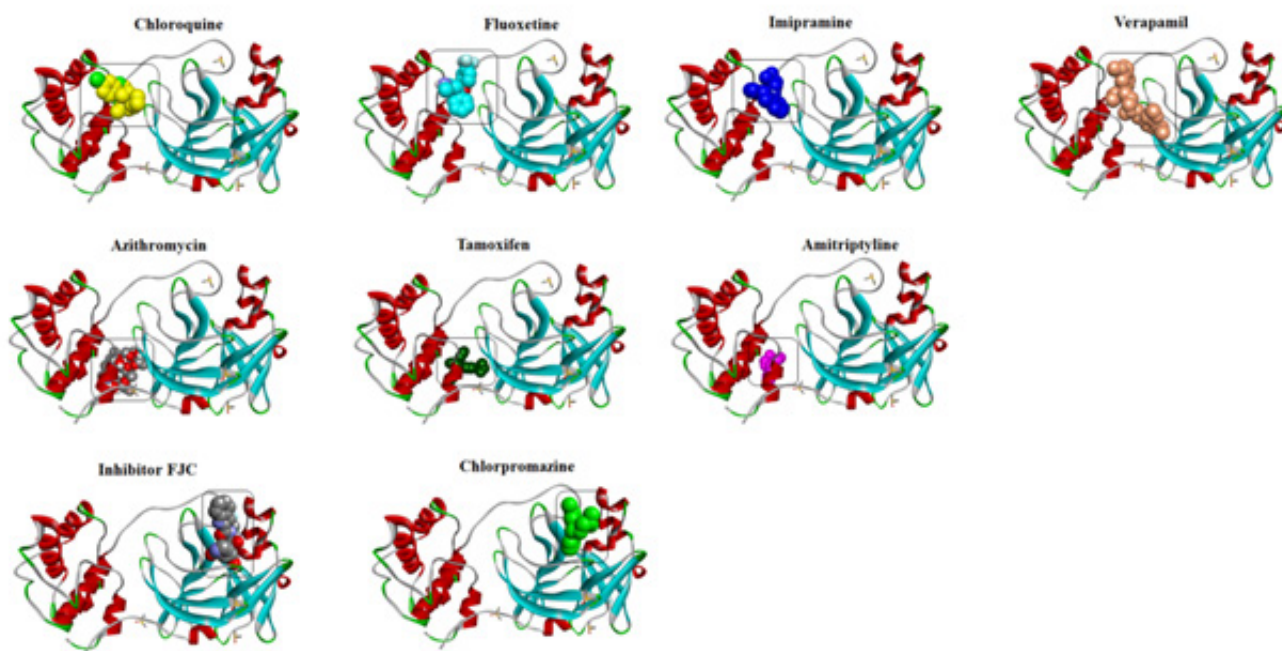


Table 2. Distances between the Mpro COVID-19 residues and the ligand

COVID-19 (Mpro) residue	Azithromycin ^b	Inhibitor FIC ^b	Remdesivir ^b	Chloroquine ^{b,c}	Fluoxetine ^c	Imipramine ^c	Verapamil ^c	Chlorpromazine ^c	Amitriptyline ^c	Tamoxifen ^c
Lys5	DNI ^d	DNI	3.23	DNI	DNI	DNI	DNI	DNI	DNI	DNI
Arg131	DNI	DNI	DNI	DNI	DNI	3.67 Å	DNI	DNI	DNI	DNI
Lys137	DNI	DNI	3.54	3.53 Å	DNI	3.70 Å	3.72 Å	DNI	DNI	DNI
Asp197	DNI	DNI	DNI	DNI	2.52 Å	4.93 Å	DNI	DNI	DNI	DNI
Thr199	DNI	DNI	DNI	DNI	3.61 Å	3.30 Å	DNI	DNI	DNI	DNI
Asn238	DNI	DNI	DNI	DNI	2.72 Å	DNI	DNI	DNI	DNI	DNI
Leu286	DNI	DNI	DNI	DNI	DNI	3.54 Å	3.88 Å	DNI	DNI	DNI
Glu288	DNI	DNI	2.48	DNI	DNI	DNI	5.28 Å	DNI	DNI	DNI
Asp289	DNI	DNI	1.86	2.35 Å	DNI	DNI	DNI	DNI	DNI	DNI
Glu290	DNI	DNI	3.23	3.98 Å	3.91 Å	DNI	5.38 Å	DNI	DNI	DNI
His41	DNI	DNI	DNI	DNI	DNI	DNI	DNI	DNI	DNI	DNI
Glu140	DNI	DNI	DNI	DNI	DNI	DNI	DNI	3.90 Å	DNI	DNI
Gly143	DNI	2.56 Å	DNI	DNI	DNI	DNI	DNI	DNI	DNI	DNI
Ser144	DNI	3.45 Å	DNI	DNI	DNI	DNI	DNI	DNI	DNI	DNI
Cys145	DNI	1.93 Å	DNI	DNI	DNI	DNI	DNI	DNI	DNI	DNI
His164	DNI	2.36 Å	DNI	DNI	DNI	DNI	DNI	DNI	DNI	DNI
Met165	DNI	3.88 Å	DNI	DNI	DNI	DNI	DNI	DNI	DNI	DNI
Glu166	DNI	1.83 Å	DNI	DNI	DNI	DNI	DNI	DNI	DNI	DNI
Pro168	DNI	DNI	DNI	DNI	DNI	DNI	DNI	DNI	DNI	DNI
Gln189	DNI	3.03 Å	DNI	DNI	DNI	DNI	DNI	DNI	DNI	DNI
Gln110	2.40 Å	DNI	DNI	DNI	DNI	DNI	DNI	DNI	DNI	DNI
Asp153	DNI	DNI	DNI	DNI	DNI	DNI	DNI	DNI	DNI	4.37 Å
Tyr154	3.93 Å	DNI	DNI	DNI	DNI	DNI	DNI	DNI	DNI	DNI
Ile249	3.67 Å	DNI	DNI	DNI	DNI	DNI	DNI	DNI	3.55 Å	3.60 Å
Pro252	DNI	DNI	DNI	DNI	DNI	DNI	DNI	DNI	3.58 Å	DNI
Pro293	3.65 Å	DNI	DNI	DNI	DNI	DNI	DNI	DNI	3.61 Å	DNI
Phe294	3.59 Å	DNI	DNI	DNI	DNI	DNI	DNI	DNI	3.98 Å	3.58 Å
Phe294	3.58 Å	DNI	DNI	DNI	DNI	DNI	DNI	DNI	DNI	DNI
Val297	DNI	DNI	DNI	DNI	DNI	DNI	DNI	DNI	3.67 Å	3.64 Å

a. The crystal structure of COVID-19 main protease - PDB ID: 6LU7 b. Molecules ligands of COVID-19 main protease described in literature. c. Lysosomotropic compounds d. **DNI**: Do Not Interact

Figure 2. Molecular interactions of the lysosomotropic compounds with the Mpro COVID-19 residues.

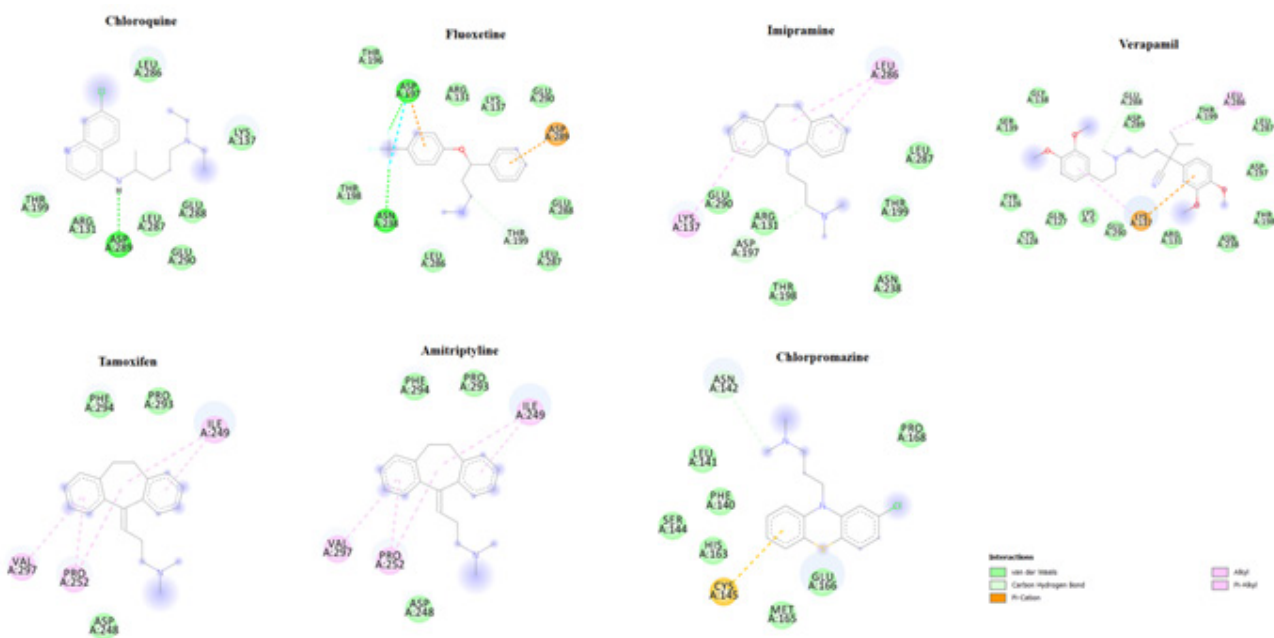


Table 3. Molecular interactions of the lysosomotropic compounds with the Mpro COVID-19 residues.

CHLOROQUINE					
Hydrophobic Interactions	COVID-19 (Mpro) residue a	Distance	-	Ligand Atom	Protein Atom
	Lys137	3.70 Å	-	16	1333
	Glu290	3.98 Å	-	15	2750
Hydrogen Bonds	COVID-19 (Mpro) residue	Distance H-A	Classification ^b	Donor Atom	Acceptor Atom
	Lys137	3.53 Å	Weak	1335 [N3+]	3 [N3]
	Asp289	2.35 Å	Average	2 [Np1]	2742 [O.co2]
FLUOXETINE					
Hydrophobic Interactions	COVID-19 (Mpro) residue	Distance	-	Ligand Atom	Protein Atom
	Asp197	3.74 Å	-	3	1873
	Thr199	3.61 Å	-	18	405
	Glu290	3.91 Å	-	15	2750
Hydrogen Bonds	COVID-19 (Mpro) residue	Distance H-A	Classification	Donor Atom	Acceptor Atom
	Asn238	2.72 Å	Strong	2	405
	Asn238	2.73 Å	Strong	1	405
Halogen(fluorine) Interactions	COVID-19 (Mpro) residue	Distance	-	-	-
	Asp197	2.52 Å	-	-	-
	Asp197	3.08 Å	-	-	-
IMIPRAMINE					
Hydrophobic Interactions	COVID-19 (Mpro) residue	Distance	-	Ligand Atom	Protein Atom
	Lys137	3.70 Å	-	9	1331
	Leu286	3.54 Å	-	5	2712
Hydrogen Bonds	COVID-19 (Mpro) residue	Distance H-A	Classification	Donor Atom	Acceptor Atom

6 Virtual screening based on molecular docking of lysosomotropic compounds for COVID-19

	Arg131	3.67 Å	Weak	1270 [Ng+]	2 [N3]
	Thr199	3.33 Å	Weak	1891 [O3]	2 [N3]
Salt Bridges	COVID-19 (Mpro) residue	Distance	-	Ligand Group	Ligand Atoms
	Asp 197	4.93 Å	-	Tertamine	2
VERAPAMIL					
Hydrophobic Interactions	COVID-19 (Mpro) residue	Distance	-	Ligand Atom	Protein Atom
	Lys137	3.72 Å	-	16	1343
	Leu286	3.88 Å	-	13	2724
π -Cation Interactions	COVID-19 (Mpro) residue	Distance	-	Ligand Group	Ligand Atoms
	Lys137	4.26 Å	-	Aromatic	4, 5, 6, 7, 8, 9
Salt Bridges	COVID-19 (Mpro) residue	Distance	-	Ligand Group	Ligand Atoms
	Glu288	5.28 Å	-	Tertamine	2
	Glu290	5.38 Å	-	Tertamine	2
CHLORPROMAZINE					
Hydrophobic Interactions	COVID-19 (Mpro) residue	Distance	-	Ligand Atom	Protein Atom
	Phe140	3.90 Å	-	12	1355
	Glu166	3.56 Å	-	8	1597
AMITRIPTYLINE					
Hydrophobic Interactions	COVID-19 (Mpro) residue	Distance	-	Ligand Atom	Protein Atom
	Ile249	3.96 Å	-	5	2395
	Ile249	3.55 Å	-	15	2396
	Pro252	3.58 Å	-	11	2418
	Pro293	3.71 Å	-	14	2778
	Phe294	3.98 Å	-	12	2785
	Val297	3.67 Å	-	13	2815
TAMOXIFEN					
Hydrophobic Interactions	COVID-19 (Mpro) residue	Distance	-	Ligand Atom	Protein Atom
	Ile249	3.92 Å	-	12	2402
	Ile249	3.60 Å	-	16	2404
	Phe294	3.85 Å	-	7	2795
	Val297	3.88 Å	-	21	2822
	Val297	3.64 Å	-	20	2823
Salt Bridges	COVID-19 (Mpro) residue	Distance	-	Ligand Group	Ligand Atoms
	Asp153	4.37 Å	-	Tertamine	1

a. The crystal structure of COVID-19 main protease - PDB ID: 6LU7

b. Hydrogen bond classification: $2,5 \text{ \AA} < d < 3,1 \text{ \AA} \Rightarrow$ Strong interaction; $3,1 \text{ \AA} < d < 3,55 \text{ \AA} \Rightarrow$ Average interaction; $d > 3,55 \text{ \AA} \Rightarrow$ Weak interaction.

Interactions of lysosomotropic compounds with the NSP16-NSP10 heterodimer of COVID-19

Regarding the second target, the interaction between the lysosomotropic molecules and the heterodimer of NSP16-NSP10 resulted in an RMSD variation of 0.735 to 1.562 Å and free binding energy of -6.0 to -8.7 kcal/mol (Table 4). Analysis of the molecular docking simulations showed that all the inhibitors bonded at the same site as the enzyme, but they were distant from the binding site of the complexed sinefungin inhibitor (SFG) (Figure 3). The amitriptyline inhibitor (Figure 3A) showed ten interactions with the heterodimer of NSP16-NSP10, all of which were hydrophobic, with the amino acids Leu6820 (3.47 Å), Tyr7020 (3.66 Å; 3.66 Å; 3.63 Å; 3.72 Å; 3.78 Å; 3.50 Å; 3.92 Å; 3.55 Å) and Val7021 (3.70 Å) (Table 3). Analysis of the receptor-ligand complex formed with chloroquine (Figure 3) revealed eight interactions in the binder with the heterodimer NSP16-NSP10, all of which were hydrophobic, with Leu6820 (3.86 Å) and Tyr7020 (3.82 Å; 3.48 Å; 3.55 Å; 3.71 Å; 3.84 Å; 3.67 Å; 3.91 Å) (Table 5). Chlorpromazine molecular docking routines (Figure 3C) showed the formation of five protein target interactions, all hydrophobic, with Leu6820 (3.80 Å), Tyr7020 (3.59 Å; 3.73 Å; 3.64 Å), and Val7021 (3.59 Å) (Table 3). Analysis of interactions with fluoxetine showed that the simulation of the molecular fit of the inhibitor (Figure 3) resulted in the formation of six interactions with the enzyme, all of them

hydrophobic, with the residues Leu6819 (3.72 Å), Tyr7020 (3.58 Å; 3.71 Å; 3.67 Å; 3.53 Å) and Val7021 (3.86 Å) (Table 5). Considering the interactions between imipramine (Figure 3) and the heterodimer NSP16-NSP10, there were seven hydrophobic interactions, with Leu6820 (3.65 Å; 3.40 Å) and Tyr7020 (3.52 Å; 3.58 Å; 3.69 Å; 3.88 Å; 3.57 Å) (Table 5). Tamoxifen (Figure 3) had eight interactions with the heterodimer NSP16-NSP10, all hydrophobic, with Leu6819 (3.70 Å), Leu6820 (3.51 Å), and Tyr7020 (3.50 Å; 3.46 Å; 3.91 Å; 3.66 Å; 3.84 Å; 3.54 Å) (Table 3). Verapamil (Figure 2) had eight interactions with the heterodimer NSP16-NSP10 of the COVID-19 virus, all of which were hydrophobic, with Leu6820 (3.86 Å), Tyr7020 (3.54 Å; 3.80 Å; 3.76 Å; 3.67 Å; 3.68 Å; 3.66 Å) and Ala7024 (3.87 Å) (Table 3).

Figure 3. The lysosomotropic compounds fluoxetine, imipramine, chloroquine, verapamil, tamoxifen, amitriptyline and chlorpromazine binding the NSP16-NSP10 SARS COV 2 residues compared to sinefungin

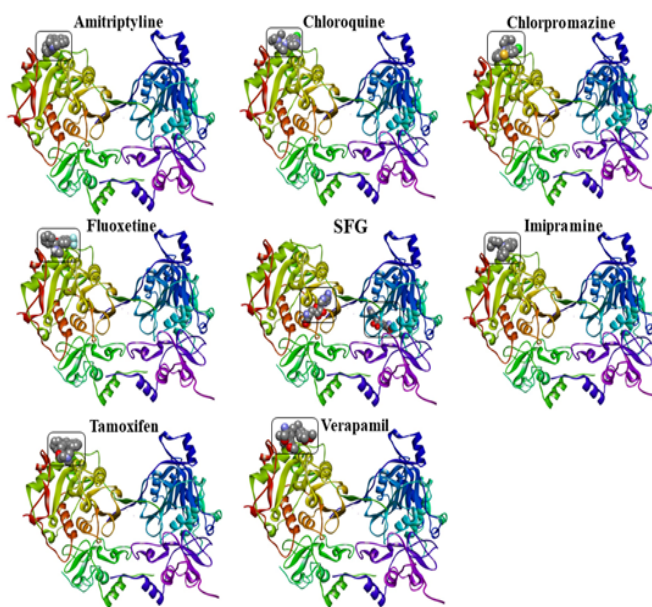


Table 4. RMSD and affinity energy values calculated in molecular docking simulations by lysosomotropic compounds in NSP16-NSP10 Heterodimer from SARS-CoV-2 residues.

Inhibitor b	Affinity (kcal/mol)	RMSD (Å)
Chloroquine	-6.0	1.322
Fluoxetine	-6.7	1.562
Imipramine	-7.1	1.271
Verapamil	-6.5	1.179
Chlorpromazine	-6.2	1.547
Amitriptyline	-8.7	0.769
Tamoxifen	-8.2	0.735

Table 5. Molecular interactions of the lysosomotropic compounds with the NSP16-NSP10 Heterodimer from SARS-CoV-2 residues.

Hydrophobic Interactions	CHLOROQUINE			
	COVID-19 (NSP16-NSP10) residue a	Distance	Ligand Atom	Protein Atom
	Leu6820	3.86 Å	14	240
	Tyr7020	3.82 Å	6	2203
	Tyr7020	3.48 Å	16	2193
	Tyr7020	3.55 Å	5	2199
	Tyr7020	3.71 Å	8	2195
	Tyr7020	3.84 Å	10	2201

8 Virtual screening based on molecular docking of lysosomotropic compounds for COVID-19

	Tyr7020	3.67 Å	11	2200
	Val7021	3.91 Å	19	2219
FLUOXETINE				
Hydrophobic Interactions	COVID-19 (NSP16-NSP10) residue a	Distance	Ligand Atom	Protein Atom
	Leu6819	3.72 Å	15	230
	Tyr7020	3.58 Å	10	2190
	Tyr7020	3.71 Å	8	2199
	Tyr7020	3.67 Å	3	2196
	Tyr7020	3.53 Å	4	2200
	Val7021	3.86 Å	10	2219
IMIPRAMINE				
Hydrophobic Interactions	COVID-19 (NSP16-NSP10) residue a	Distance	Ligand Atom	Protein Atom
	Leu6820	3.65 Å	16	238
	Leu6820	3.40 Å	14	235
	Tyr7020	3.52 Å	10	2191
	Tyr7020	3.58 Å	8	2197
	Tyr7020	3.69 Å	7	2194
	Tyr7020	3.88 Å	9	2192
	Tyr7020	3.57 Å	15	2198
VERAPAMIL				
Hydrophobic Interactions	COVID-19 (NSP16-NSP10) residue a	Distance	Ligand Atom	Protein Atom
	Leu6820	3.86 Å	8	250
	Tyr7020	3.54 Å	7	2209
	Tyr7020	3.80 Å	14	2200
	Tyr7020	3.76 Å	26	2206
	Tyr7020	3.67 Å	15	2204
	Tyr7020	3.68 Å	22	2214
	Tyr7020	3.66 Å	20	2210
	Ala7024	3.87 Å	14	2256
Salt Bridges	COVID-19 (NSP16-NSP10) residue a	Distance	Ligand Group	Ligand Atoms
	Asp7018	3.70 Å	Tertamine	2
CHLORPROMAZINE				
Hydrophobic Interactions	COVID-19 (NSP16-NSP10) residue a	Distance	Ligand Atom	Protein Atom
	Leu6820	3.80 Å	10	235
	Tyr7020	3.59 Å	9	2201
	Tyr7020	3.73 Å	8	2191
	Tyr7020	3.64 Å	7	2194
	Val7021	3.59 Å	8	2217

Salt Bridges	COVID-19 (NSP16-NSP10) residue a	Distance	Ligand Group	Ligand Atoms
	Asp7018	4.71 Å	Tertamine	2
AMITRIPTYLINE				
Hydrophobic Interactions	COVID-19 (NSP16-NSP10) residue a	Distance	Ligand Atom	Protein Atom
	Leu6820	3.47 Å	18	235
	Tyr7020	3.66 Å	17	2188
	Tyr7020	3.66 Å	9	2191
	Tyr7020	3.63 Å	11	2197
	Tyr7020	3.72 Å	21	2200
	Tyr7020	3.78 Å	10	2194
	Tyr7020	3.50 Å	20	2202
	Tyr7020	3.92 Å	12	2192
	Tyr7020	3.55 Å	13	2198
	Val7021	3.70 Å	16	2217
TAMOXIFEN				
Hydrophobic Interactions	COVID-19 (NSP16-NSP10) residue a	Distance	Ligand Atom	Protein Atom
	Leu6819	3.70 Å	15	235
	Leu6820	3.51 Å	7	245
	Tyr7020	3.50 Å	23	2208
	Tyr7020	3.46 Å	18	2204
	Tyr7020	3.91 Å	21	2207
	Tyr7020	3.66 Å	19	2201
	Tyr7020	3.84 Å	20	2209
	Tyr7020	3.54 Å	11	2199

a. The crystal structure of COVID-19 main protease - PDB ID: 6LU7

b. Hydrogen bond classification: $2,5 \text{ \AA} < d < 3,1 \text{ \AA} \Rightarrow$ Strong interaction; $3,1 \text{ \AA} < d < 3,55 \text{ \AA} \Rightarrow$ Average interaction; $d > 3,55 \text{ \AA} \Rightarrow$ Weak interaction

DISCUSSION

The term lysosomotropic was initially introduced by²³, who originally proposed it for all substances selectively absorbed by lysosomes. These molecules have the characteristic of accumulating in acidic compartments, so they can pass through the membrane neutrally. However, when they reach a more acidic environment, their protonation occurs and they can no longer return through the membrane²⁴. In this sense, lysosomotropic agents act to inhibit endosomal maturation and cause the interruption of endolysosomal traffic. These effects are particularly relevant in the context of viral infection, possibly resulting from pH modulation and interaction with molecular systems involved in regulating the pH of lysosomal vesicles [25]. In this context, due to the lack of effective strategies against COVID-19, the repositioning of drugs based on their lysosomotropic and endolysosomal pH modulating effects

may provide additional options for therapy and prevention²⁵. According to²⁶, because these substances act in various events during SARS-CoV-2 infection and disease progress, they constitute a promising approach.

The results obtained from the evaluation carried out in this study demonstrated the interactions between the compounds analyzed with Mpro COVID-19, one of the proteases responsible for the processing and release of non-structural proteins (NSPs)^{2,27}, a target that has been used for in silico study to find substances that can inhibit SARS-CoV-2^{2,28,29}. At this juncture, understanding the intermolecular forces is a key point for understanding how chemical systems behave at the molecular level³⁰.

Thus, regarding the results of the analysis with Mpro COVID-19, fluoxetine (Asn238) and imipramine (Arg131 and Thr199) exhibited hydrogen bond interactions, playing an important role in the structure and function of biomolecules³¹, the reason they are frequently used in drug design³². In addition, fluoxetine (Asp197, Thr199, and Glu290), imipramine (Lys137 and Leu286), verapamil (Lys137 and Leu286), tamoxifen (Ile249, Phe294, and Val297), amitriptyline (Ile249, Pro252, Pro293, Phe294, and Val297) and chlorpromazine (Phe140 and Glu166) presented hydrophobic interactions. Due to the importance of these interactions in drug design through stabilization of binders and increase of binding affinity at the target-drug interface³³, they need to be further investigated.

Other types of interactions were also observed concerning the analysis with Mpro COVID-19, such as π -cation interactions with verapamil (Lys137), salt bridge interactions with imipramine (Asp197), verapamil (Glu288 and Glu290), and tamoxifen (Asp153), and halogen (fluorine) interactions with fluoxetine (Asp197), also useful in the context of targeted drug design³⁴. According to³⁵, hydrogen bonds, salt bridges, and halogen bonding are practical and effective tools used by medicinal chemists to rationally design molecular entities that have high power to bond to a given target. Thus, because of the good knowledge about the structural, geometric, energetic, and thermodynamic properties related to these non-covalent interactions in ligand-protein complexes, they have promise for the design of new agents against diseases. In addition, π -cation interactions are important for molecular recognition, coupled with hydrophobic effects, hydrogen bonding, and ionic pairing, both for the determination of macromolecular structures and interactions in drug receptors³⁶.

Moreover, an analysis of the interactions between the compounds under study with NSP16-NSP10 was performed. They all formed protein complexes that acted by catalyzing the methylation of the penultimate nucleotide in the viral RNA cap at position 2'-O of ribose³⁷, an important target associated with viral replication^{38,39}. In general, all drugs tested had hydrophobic interactions with the target protein, varying depending on the residues involved. They were the same for amitriptyline and chlorpromazine (Leu6820, Tyr7020, and Val7021), and for chloroquine and imipramine (Leu6820 and Tyr7020), but different in the residues for fluoxetine (Leu6819, Tyr7020, and Val7021), tamoxifen (Leu6819, Leu6820, and Tyr7020) and verapamil (Leu6820, Tyr7020, and Ala7024).

In the *in silico* study performed by⁴⁰, the activity of several compounds on NSP10-NSP16 and Mpro of SARS-CoV-2 was analyzed, and the authors found that hydrophobic and hydrogen bond interactions played significant roles in predicting protein-ligand affinity with these targets. Our results corroborate those findings. It is worth noting that hydrophobic interactions occurred in all compounds analyzed for NSP10-

NSP16 in this study so that this type of interaction indicates specific functional groups that may be responsible for the effect of hydrophobic generation, with strong binding affinity against the target proteins, thus having an important influence on the infection caused by SARS-CoV-2⁴⁰.

As far as the free binding energy is concerned, the value considered as standard in the literature is -6.0 kcal/mol or less⁷. From this, we found that the lysosomotropic compounds under study obtained better results related to this parameter in the analysis performed with the NSP10-NSP16 heterodimer, with variation from -6.0 to -8.7 kcal/mol, while for Mpro, the variation occurred in the range of -4.2 to -6.7 kcal/mol, not showing adequate binding energy.

Some drugs investigated in this study are already included in clinical trials for evaluation against COVID-19 (clinicaltrials.gov), such as chloroquine, chlorpromazine, azithromycin, fluoxetine, tamoxifen, and verapamil, given the potential pH-mediated endolysosomal effect on SARS-CoV-2, as reported in the review of²⁵ for azithromycin and fluoxetine. Thus, we stress the relevance of further analyzing these drugs to elucidate the molecular aspects involved in the interaction with important targets in SARS-CoV-2.

CONCLUSION

In the molecular docking analysis of the lysosomotropic compounds fluoxetine, imipramine, chloroquine, verapamil, tamoxifen, amitriptyline, and chlorpromazine with the main protease of COVID-19, it was observed that all the ligands presented a greater distance from the inhibitors (remdesivir, azithromycin, and FIC inhibitor) complexed in Mpro, bonded to distinct regions of the enzyme. Regarding the study against the NSP16-NSP10 heterodimer, all the ligands bonded at the same site as the enzyme, but they were far from the binding site of the complexed simefungin inhibitor (SFG). About the interactions, hydrophobic, hydrogen bonds, salt bridges, halogen bonding and π -cation for Mpro, and hydrophobic for heterodimer NSP16-NSP10, were verified, with a different pattern of interaction for most compounds. Concerning the free binding energy, the drugs showed better results with the NSP16-NSP10 heterodimer, demonstrating values within the standard considered in the literature. Thus, this study elucidates the molecular aspects involved with potential drugs in important targets for SARS-CoV-2, so that these results can serve as a basis for the development of new antiviral drugs in the context of drug repositioning.

ACKNOWLEDGMENTS

This research was supported by grants and fellowships from CNPq, CAPES/Brazil, and FUNCAP/Ceará. We declare no conflicts of interest concerning this article.

REFERENCES

- Hall DC Jr, Ji H-F. A search for medications to treat COVID-19 via in silico molecular docking models of the SARS-CoV-2 spike glycoprotein and 3CL protease. *Travel Med Infect Dis* [Internet]. 2020 May-Jun; 35: 101646. doi: <https://doi.org/10.1016/j.tmaid.2020.101646>.
- Kandeel M, Al-Nazawi M. Virtual screening and repurposing of FDA approved drugs against COVID-19 main protease. *Life Sci* [Internet]. 2020 Jun; 251: 117627. doi: <https://doi.org/10.1016/j.lfs.2020.117627>.
- Rothan HA, Byrareddy SN. The epidemiology and pathogenesis of coronavirus disease (COVID-19) outbreak. *J Autoimmun* [Internet]. 2020 May; 109: 102433. doi: <https://doi.org/10.1016/j.jaut.2020.102433>.
- Joshi T, Sharma P, Joshi T, Pundir H, Mathpal S, Chandra S. Structure-based screening of novel lichen compounds against SARS Coronavirus main protease (Mpro) as potential inhibitors of COVID-19. *Mol Divers* [Internet]. 2021 Aug; 25(3): 1665-1677. doi: <http://link.springer.com/10.1007/s11030-020-10118-x>.
- Zheng Y, Shang J, Yang Y, Liu C, Wan Y, Geng Q, et al. Lysosomal Proteases Are a Determinant of Coronavirus Tropism. *J Virol*. 2018 Nov; 92(24): e01504-18. doi: 10.1128/JVI.01504-18.
- Lu S, Sung T, Lin N, Abraham RT, Jessen BA. Lysosomal adaptation: How cells respond to lysosomotropic compounds. *PLoS One*. 2017 Mar; 12(3): 0173771. doi: 10.1371/journal.pone.0173771.
- Marinho EM, Batista de Andrade Neto J, Silva J, Rocha da Silva C, Cavalcanti BC, Marinho ES, et al. Virtual screening based on molecular docking of possible inhibitors of Covid-19 main protease. *Microb Pathog* [Internet]. 2020 Nov; 148: 104365. doi: 10.1016/j.micpath.2020.104365.
- Jin Z, Du X, Xu Y, Deng Y, Liu M, Zhao Y, et al. Structure of Mpro from COVID-19 virus and discovery of its inhibitors. *Nature*. 2020 Jun; 582(7811): 289-293. doi: 10.1038/s41586-020-2223-y.
- Guerra TM. Estudos de Docking Molecular de Derivados da Tiazolidina Como Potenciais Inibidores da Enzima Cruzaina de *Trypanosoma cruzi* [TCC]. Serra Talhada (PE): Universidade Federal Rural de Pernambuco/ Unidade Acadêmica de Serra Talhada-PE; 2019.
- Lucio FNM, Da Silva JE, Marinho EM, Mendes FRDS, Marinho MM, Marinho ES. Methylcytosine alkaloid potentially active against dengue virus: A molecular docking study and electronic structural characterization. *Int J Res-Granthaalayah*. 2020;8(1):221-36.
- Milite C, Amendola G, Nocentini A, Bua S, Cipriano A, Barresi E, et al. Novel 2-substituted-benzimidazole-6-sulfonamides as carbonic anhydrase inhibitors: synthesis, biological evaluation against isoforms I, II, IX and XII and molecular docking studies. *J Enzyme Inhib Med Chem*. 2019; 34(1): 1697-710. doi: 10.1080/14756366.2019.1666836.
- Dewar MJS, Zoebisch EG, Healy EF, Stewart JJP. Development and use of quantum mechanical molecular models. *J Am Chem Soc*. 1985; 107(13): 3902-3909.
- Bani-Yaseen AD. Computational molecular perspectives on the interaction of propranolol with β -cyclodextrin in solution: Towards the drug-receptor mechanism of interaction. *J Mol Liq*. 2017 Feb; 227: 280-90. doi: <https://doi.org/10.1016/j.molliq.2016.12.023>.
- Stewart JJP. Optimization of parameters for semiempirical methods V: Modification of NDDO approximations and application to 70 elements. *J Mol Model*. 2007 Dec; 13(12): 1173-1213. doi: 10.1007/s00894-007-0233-4.
- Stewart JJP. Optimization of parameters for semiempirical methods VI: More modifications to the NDDO approximations and re-optimization of parameters. *J Mol Model*. 2013 Jan; 19(1): 1-32.
- Dral PO, Wu X, Spörkel L, Koslowski A, Weber W, Steiger R, et al. Semiempirical quantum-chemical orthogonalization-corrected methods: theory, implementation, and parameters. *J Chem Theory Comput*. 2016;12:1082-96. doi: <https://doi.org/10.1021/acs.jctc.5b01046>.
- Arroio A, Honório KM, Da Silva ABF. Propriedades químico-quânticas empregadas em estudos das relações estrutura-atividade. *Quim Nova*. 2010; 33(3): 694-9. doi: <https://doi.org/10.1590/S0100-40422010000300037>.
- Trott O, Olson AJ. Software News and Update AutoDock Vina : Improving the Speed and Accuracy of Docking with a New Scoring Function , Efficient Optimization , and Multithreading. *J Comput Chem*; 2010 Jan; 31(2): 455-61. doi: 10.1002/jcc.21334.
- Yusuf D, Davis AM, Kleywegt GJ, Schmitt S. An Alternative Method for the Evaluation of Docking Performance : RSR vs RMSD. 2008 Jul;148: 411-22. doi: <https://doi.org/10.1021/ci800084x>.
- Shityakov S, Förster C. In silico predictive model to determine vector-mediated transport properties for the blood-brain barrier choline transporter. *Adv Appl Bioinforma Chem*. 2014 Sep; 7: 23-36. doi: 10.2147/AABC.S63749.
- Petterson EF, Goddard TD, Huang CC, Couch GS, Greenblatt DM, Meng EC, et al. UCSF Chimera - - A Visualization System for Exploratory Research and Analysis. 2004 Oct; 25(13): 1605-12. doi: 10.1002/jcc.20084.
- Jonathan W. Steed JLA. *Supramolecular Chemistry*. 2nd ed. Wiley; 2009.
- Duve C, Barsey T, Poole B, Trouret A, Tulkens P, Van Hoof F. Lysosomotropic agents. *Biochem Pharmacol*. 1974; 23(18): 2495-531. doi: 10.1016/0006-2952(74)90174-9.
- Norinder U, Tuck A, Norgren K, Munic Kos V. Existing highly accumulating lysosomotropic drugs with potential for repurposing to target COVID-19. *Biomed Pharmacother*. 2020 Oct; 130: 110582. doi: 10.1016/j.biopha.2020.110582.
- Homolak J, Kodvanj I. Widely available lysosome targeting agents should be considered as potential therapy for COVID-19. *Int J Antimicrob Agents*. 2020 Aug; 56(2): 106044. doi: 10.1016/j.ijantimicag.2020.106044.
- Blaess M, Kaiser L, Sauer M, Csuk R, Deigner HP. COVID-19/SARS-CoV-2 infection: Lysosomes and lysosomotropism implicate new treatment strategies and personal risks. *Int J Mol Sci*. 2020 Jul; 21(14): 4953. doi: 10.3390/ijms21144953.
- Hilgenfeld R. From SARS to MERS: crystallographic studies on coronavirus proteases enable antiviral drug design. *FEBS J*. 2014 Sep; 281(18): 4085-96. doi: 10.1111/febs.12936.
- Khan RJ, Jha RK, Amara GM, Jain M, Singh E, Pathak A, et al. Targeting SARS-CoV-2: a systematic drug repurposing approach to identify promising inhibitors against 3C-like proteinase and 2'-O-ribose methyltransferase. *J Biomol Struct Dyn*. Taylor & Francis; 2020 Apr; 39(8):1-14.
- Kouligi S, Jani V, Uppuladinne M, Sonavane U, Nath AK, Darbari H, et al. Drug repurposing studies targeting SARS-CoV-2: an ensemble docking approach on drug target 3C-like protease (3CLpro). *J Biomol Struct Dyn*. 2020 Sep; 39(15): 5735-5755. doi: 10.1080/07391102.2020.1792344.
- Pinheiro S, Soteras I, Gelpí JL, Dehez F, Chipot C, Luque FJ, et al. Structural and energetic study of cation- π -cation interactions in proteins. *Phys Chem Chem Phys*. 2017 Mar; 19: 9849-61.
- Jeffrey GA, Saenger W. *Hydrogen Bonding in Biological Structures*. Springer Berlin Heidelberg; 2012.
- Klaholz BP, Moras D. C-H \cdots O hydrogen bonds in the nuclear receptor RAR γ - A potential tool for drug selectivity. *Structure*. 2002 Sep; 10(9): 1197-204.

12 Virtual screening based on molecular docking of lysosomotropic compounds for COVID-19

33. Patil R, Das S, Stanley A, Yadav L, Sudhakar A, Varma AK. Optimized hydrophobic interactions and hydrogen bonding at the target-ligand interface leads the pathways of Drug-Designing. *PLoS One*. 2010 Aug; 5(8): e12029. doi: 10.1371/journal.pone.0012029.
34. Sirimulla S, Bailey JB, Vegesna R, Narayan M. Halogen interactions in protein-ligand complexes: Implications of halogen bonding for rational drug design. *J Chem Inf Model*. 2013 Nov; 53(11): 2781–91. doi: 10.1021/ci400257k.
35. Zhou P, Huang J, Tian F. Specific Noncovalent Interactions at Protein-Ligand Interface: Implications for Rational Drug Design. *Curr Med Chem*. 2012; 19(2): 226–38. doi: 10.2174/092986712803414150.
36. Dougherty DA. The cation- π interaction. *Acc Chem Res*. 2013 Apr. ;46:885–93. doi: 10.1021/ar300265y.
37. Lin S, Chen H, Ye F, Chen Z, Yang F, Zheng Y, et al. Crystal structure of SARS-CoV-2 nsp10/nsp16 2'-O-methylase and its implication on antiviral drug design. *Signal Transduct Target Ther*. 2020 Jul; 5(1): 131. doi: 10.1038/s41392-020-00241-4.
38. Vidyasagar V. Clinical Evidence of Possible Drug Targets and Pharmacological Management of Novel Covid-19 : The World Threatening Virus. *Adv Clin Pharmacol Toxicol Ther*. 2019;1:1–6. (LINK DE ACESSO: https://d1wqtxts1xle7.cloudfront.net/63887870/ACPTT-1-11120200710-87650-1d77sh1-with-cover-page-v2.f?Expires=1653498333&Signature=HaZFudtiVSLD43Zvw2yntDbUKHXurTBHY5gQsfd7pVJ5dkJRwbkgW77~00jLTIGHEIOBG20IFuRms hxupMJ~8ce7Uao8qdsL6rdKJHZ1npc2qSW4Zpq8oHtoAOVgoXmeSSBcz2xrg9LgnBjvNUhnsxuJeUf~D85Tdcz~pCHf6Umxk12LIING-EDp6EmefypLdte-FDVao6URnJ~8A-i7xqwRkT4-v-W9vdMJErzACcaNa7~9oneeuF9W2zWtfsKfQpzpfzCRi5Uuhnz-ZaFgJJ19TITjON7kLtmGMVvuULOxMl6bPiofr9mT-69~uDyWFqYpluU5prMeiLiNoXwA__&Key-Pair-Id=APKAJLOHF5GGSLRBV4ZA)
39. Wang Y, Sun Y, Wu A, Xu S, Pan R, Zeng C, et al. Coronavirus nsp10/nsp16 Methyltransferase Can Be Targeted by nsp10-Derived Peptide In Vitro and In Vivo To Reduce Replication and Pathogenesis . *J Virol*. 2015 Aug; 89(16): 8416–27. doi: 10.1128/JVI.00948-15.
40. Maurya SK, Maurya AK, Mishra N, Siddique HR. Virtual screening, ADME/T, and binding free energy analysis of anti-viral, anti-protease, and anti-infectious compounds against NSP10/NSP16 methyltransferase and main protease of SARS CoV-2. *J Recept Signal Transduct Res*. 2020: 1–8. doi: 10.1080/10799893.2020.1772298.

Como citar este artigo/ How to cite this article:

Andrade JB Neto, Marinho EM, Silva CR, Sá LGAV, Cabral VPF, Cândido TM et al. Virtual screening based on molecular docking of lysosomotropic compounds as therapeutic agents for COVID-19. *J Health Biol Sci*. 2022; 10(1):1-12.